

Locating Everyday Objects using NFC Textiles

Jingxian Wang*

jingxian@cmu.edu

Carnegie Mellon University
PA, USA

Chengfeng Pan

chengfep@andrew.cmu.edu
Carnegie Mellon University
PA, USA

Junbo Zhang*

junboz2@andrew.cmu.edu
Carnegie Mellon University
PA, USA

Ke Li

kl975@cornell.edu
Cornell University
NY, USA

Carmel Majidi

cmajidi@andrew.cmu.edu
Carnegie Mellon University
PA, USA

Swarun Kumar

swarun@cmu.edu
Carnegie Mellon University
PA, USA

ABSTRACT

This paper builds a Near-field Communication (NFC) based localization system that allows ordinary surfaces to locate surrounding objects with high accuracy in the near-field. While there is rich prior work on device-free localization using far-field wireless technologies, the near-field is less explored. Prior work in this space operates at extremely small ranges (a few centimeters), leading to designs that sense close proximity rather than location.

We propose TextileSense, a near-field beamforming system which can track everyday objects made of conductive materials (e.g., a human hand) even if they are a few tens of centimeters away. We use multiple flexible NFC coil antennas embedded in ordinary and irregularly shaped surfaces we interact with in smart environments – furniture, carpets, etc. We design and fabricate specialized textile coils woven into the fabric of the furniture and easily hidden by acrylic paint. We then develop a near-field blind beamforming algorithm to efficiently detect surrounding objects, and use a data-driven approach to further infer their location. A detailed experimental evaluation of TextileSense shows an average accuracy of 3.5 cm in tracking the location of objects of interest within a few tens of centimeters from the furniture.

CCS CONCEPTS

- Networks → Network services; Sensor networks;
- Human-centered computing → Ubiquitous and mobile computing design and evaluation methods.

*Both authors contributed equally to this research.

Permission to make digital or hard copies of part or all of this work for personal or classroom use is granted without fee provided that copies are not made or distributed for profit or commercial advantage and that copies bear this notice and the full citation on the first page. Copyrights for third-party components of this work must be honored. For all other uses, contact the owner/author(s).

IPSN '21, May 18–21, 2021, Nashville, TN, USA

© 2021 Copyright held by the owner/author(s).

ACM ISBN 978-1-4503-8098-0/21/05.

<https://doi.org/10.1145/3412382.3458254>

KEYWORDS

Battery-free Networks; Near-field MIMO; NFC

ACM Reference Format:

Jingxian Wang, Junbo Zhang, Ke Li, Chengfeng Pan, Carmel Majidi, and Swarun Kumar. 2021. Locating Everyday Objects using NFC Textiles. In *The 20th International Conference on Information Processing in Sensor Networks (co-located with CPS-IoT Week 2021) (IPSN '21), May 18–21, 2021, Nashville, TN, USA*. ACM, New York, NY, USA, 16 pages. <https://doi.org/10.1145/3412382.3458254>

1 INTRODUCTION

This paper seeks to build an NFC MIMO beamforming system that can accurately localize objects, with or without NFC capability in the *near-field*. While there has been rich prior work on device and device-free localization in the far-field, for instance, using technologies such as Bluetooth [8], mm-wave [24], ultrasound [21], RFID [47] and visible light [49], much less exploration exists in the near-field. However, near-field technologies have significant advantages that are worth exploring: (1) their shorter range raises less privacy implications compared to the far-field counterparts; (2) technologies such as NFC are ubiquitous in our smart phones as well as battery-free everyday objects (e.g., credit cards, ID cards, etc.). The few systems that do explore near-field localization in prior work are limited, however, in one of two key ways: (1) First, they only operate at extremely close ranges (e.g., few cm), at which point, localization reduces to proximity sensing [42]. This excludes ranges of tens of centimeters – an interesting region where both near-field and far-field effects are in play. (2) Second, most prior near-field localization systems require rigid coils that can only be mounted on regular and flat surfaces [25, 34].

This paper aims to use NFC multi-coil beamforming to detect the presence and location of certain objects of interest within tens of centimeters – where both near-field and far-field effects interplay. We seek to sense certain classes of objects made of conductive material (e.g., objects containing metal, or human hands) in close proximity (e.g., few tens of

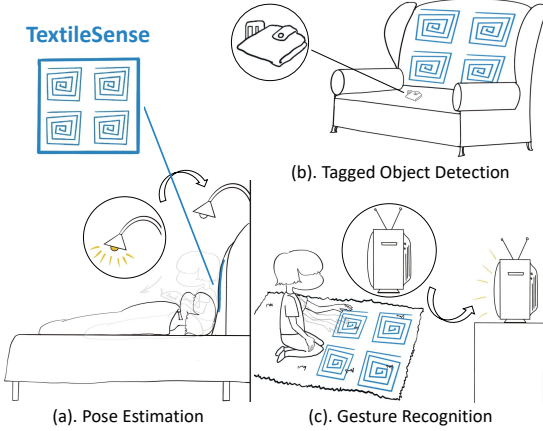


Figure 1: TextileSense can be integrated into ordinary furniture (e.g., couch, bed, or carpet). Multiple textile coils sense the presence and location of conductive objects within a few tens of centimeters. This opens up many applications: a) body posture sensing; b) Lost and found: TextileSense notifies the user where he/she left a wallet; c) user interface: the blanket serves as a touchless screen to control home appliances.

centimeters). Our system senses these objects with flexible textile-friendly coils attached to existing irregularly shaped home surfaces like a couch or a carpet. We demonstrate how this opens up several applications for human-computer interfaces, gesture, and posture sensing (see Fig. 1).

We present TextileSense – a near-field sensing system for flexible textile surfaces that senses surrounding objects made of conductive materials. TextileSense’s core includes multiple textile coil antennas that can be embedded in the furniture covering and readily hidden by puffy paints. The coils together operate as a near-field MIMO system and can manipulate the near-field to recognize objects of interest at unknown locations across farther distances. We consider two classes of objects: (1) Tagged non-conductive objects, such as NFC-enabled credit cards and key fobs, whose identity and location can be obtained; (2) Untagged conductive objects, such as human hands and metallic objects, whose presence and location can be identified. A detailed experimental evaluation on TextileSense shows a 3.6 cm accuracy in locating NFC tags with various distances and orientations and a 2.9 cm accuracy in locating human hands. We further show that TextileSense can operate accurately at a distance of 20.3 cm , a four-fold improvement over the range limit of 5 cm of commercial NFC.

TextileSense’s secret sauce is a mechanism to develop a textile NFC reader with the ability to accurately sense the location of tagged/untagged objects, within a few tens of centimeters of the furniture, regardless of their position or orientation. To do so, we rely on a familiar wireless technology:

MIMO. In far-field wireless technologies (e.g., Wi-Fi, cellular, etc.), MIMO uses multi-antenna radios to collectively beam signal power towards different spatial directions so as to improve radio coverage and enable advanced location tracking. However, developing the analogous multi-coil MIMO in the near-field poses several new challenges. First, to beam energy accurately and sense an object, one needs to know the direction; yet, for tag-free objects at unknown locations, this is unknown *a priori*, leading to a chicken-or-egg problem. Second, unlike in the traditional far-field propagation model, even if we do find the optimal beamforming direction, it may not directly relate to the location of objects. The rest of this paper describes how we solve these key challenges to enable near-field MIMO for NFC.

Detecting Objects Using Near-Field Beamforming: The first challenge is to address the chicken-or-egg problem: how to know the direction to beam RF energy without knowing the object’s location? A natural approach to do so is to apply a variety of beamforming weights and beam energy to different subsets of the space within proximity of the NFC furniture. These beamforming weights must be carefully chosen to fully cover the space around the furniture, yet minimizing the overlap between them to speed up the search. This calls for precise models on how beamforming weights in the near-field translate into the spatial patterns of energy. While such models have been explored in the far-field (e.g. in the RFID context [44]), doing so for the near-field communication is more complicated. The energized pattern is not only determined by the set of phase shifts applied across the array of NFC readers, but also impacted by the location, orientation, and impedance of the unknown objects.

To address this challenge, TextileSense develops a blind near-field beamforming algorithm to sense objects in the near-field with unknown locations, orientation, and impedance. At a high level, TextileSense uses the magnetic coupling between the object and the reader to infer the optimal beamforming weights to detect its presence, regardless of whether this object has NFC coils or is made of conductive materials. Specifically, once the object couples with the reader, it can be seen as a high impedance load to the transmitter circuit (NFC reader). In other words, the transmitter circuit should notice a voltage variation if a load is introduced into the circuit. The voltage variation will change when the load (e.g. NFC card, metal, human body, etc.) harvests more energy from the NFC readers, and this variation can be measured from the transmitter side. By leveraging this physical principle, TextileSense uses a gradient-based approach favoring the set of beamforming weights which introduce large voltage variation into the transmitter circuit. By repeating this process, our algorithm converges to the optimal set of beamforming

weights that sense the presence of objects in proximity. Sec. 4 further details our solution to detect objects.

Locating Objects in the Near-Field: Once detected, the next challenge TextileSense must address is to locate the objects of interest. A key challenge here is the limited bandwidth of NFC as well as the non-applicability of traditional far-field MIMO location tracking solutions that rely on the distance between the objects-of-interest and the reader being farther than one wavelength. To address this, our approach relies on the fact that unlike the far-field, the near-field experiences significant voltage shifts at readers due to coupling that can be reliably measured. TextileSense develops a detailed empirical model of the locations of the object based on the beamforming weights as well as the amplitude of object-related voltage response as perceived from the readers. Sec. 5 describes the details of our approach.

Building NFC-enabled Flexible Textiles: Finally, TextileSense should integrate textile-compatible coils to build NFC-enabled furniture. In collaboration with material science researchers, we present a novel solution to fabricate coils with conductive fabric, which can be woven into the furniture covering and allows for flexibility and stretchability to ensure user comfort. Sec. 6 describes how TextileSense is informed by experimentation and analysis to ensure the robustness of its textile coils when subject to bending and crumpling, and how it models the consequent resonant frequency shift and antenna gain degradation. Further, in Sec. 9, we discuss the possible security implication of TextileSense.

Applications: TextileSense opens up several applications which we briefly explain below and evaluate in Sec. 8.6:

- *Object Tracking:* TextileSense can identify and track the location of objects of interest already with an NFC coil, e.g. a credit card. This can be used to both track your credit card if it is lost, as well as track NFC-tagged objects at fine-grained accuracy in virtual reality games.
- *User Interface:* TextileSense can also serve as a user interface that transforms your furniture into a touchless screen to control your devices. We evaluate the specific application of tracking fine-grained gestures of a human hand.
- *Body Posture Estimation:* TextileSense can detect the location where the user is seated in the couch and recognize their body posture relying on the coupling between the human body and TextileSense.

Limitations: We emphasize a few important limitations of TextileSense (detailed in Sec. 9): (1) TextileSense cannot deal with extremely small spacing between multiple objects that need to be simultaneously discerned (within 1.5 mm) due to the strong coupling among them; (2) TextileSense's performance can be degraded by extreme folds or wrinkles

of textiles, and our approach explicitly designs solutions to minimize this degradation. (3) TextileSense NFC readers require a power source; however, it can readily piggyback on access to wall power commonly available in configurable furniture (e.g. reclinable couches).

We implement TextileSense on four software-defined radios, each connected to an 18 × 18 cm custom conductive Nylon-based square coil attached to the couch. Our results show:

- TextileSense achieves an average accuracy of 3.6 cm in locating passive NFC tags.
- TextileSense achieves an average accuracy of 2.9 cm in locating a human hand.
- TextileSense achieves a detection range of 20.3 cm using four software-defined radios in tracking NFC cards in close proximity, a 4 × improvement compared to commercial NFC systems.

Contributions: We propose a localization system design of a MIMO-enabled NFC reader which locates surrounding NFC tags as well as untagged conductive objects. Our system achieves few centimeter level location tracking of nearby tagged and untagged objects and an overall detection range of 20.3 cm from the textile NFC reader.

Video: https://youtu.be/Ieil0NQlk_M.

2 NFC FUNDAMENTALS

This section describes the basics of the NFC protocol and the mechanics of near-field magnetic coupling for both tagged and untagged objects.

NFC Protocol: According to the ISO 14443 NFC protocol, an NFC reader initiates communication by periodically broadcasting a universal query command to wake up nearby tags (if any) and solicit responses (standard acknowledgment and unique IDs). Meanwhile, it inevitably experiences magnetic coupling with nearby conducting objects, even if they do not contain NFC coils.

Magnetic Coupling in NFC: The underlying communication principle of NFC is based on magnetic coupling. The NFC reader operates in the 13.56 MHz ISM band. The current flowing through the coil antenna of the NFC reader generates a magnetic field that couples with nearby NFC tags or conductive untagged objects. In the rest of this discussion, we use *object* to denote either a tagged or untagged object that magnetically couples with the NFC reader – the underlying physics remains largely the same. The magnetic coupling effect transfers energy from the NFC reader to the object owing to an induced current in the object. In the near-field, since the strength of magnetic fields decreases rapidly with distance by its inverse 2–3rd power [40], the communication range of commercial NFC systems is around 5 cm.

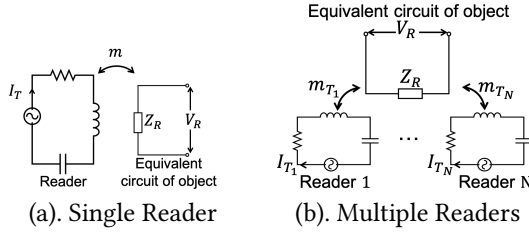


Figure 2: (a) The magnetic coupling between the active NFC reader and an object of interest can be quantified as the mutual inductance m . It induces a voltage V_R across the object’s equivalent circuit. (b) A team of reader coils couple with a tagged or untagged object.

Fig. 2 (a) shows a simplified circuit diagram for a single pair of reader and object, with the latter shown by its equivalent circuit. Due to the magnetic coupling between the reader and the object, the current I_T in the reader will induce a voltage V_R on the object:

$$V_R = Z_R I_R = m I_T \quad (1)$$

where m is the mutual inductance between the antenna of the object and the reader at the resonant frequency; Z_R and I_R are the impedance and current induced in the object’s equivalent circuit.

As the object perceives an induced voltage from the reader, the current induced also generates its own magnetic field which changes the voltage across the reader antenna. The voltage V_T across the reader antenna is written as:

$$V_T = V_0 - V'_R = V_0 - m I_R \quad (2)$$

where V'_R is the voltage introduced by the object and V_0 is the original voltage on the reader antenna without any object in range. In effect, the object functions as a voltage divider. Hence, we conclude that when there is less energy delivered to the nearby object, the voltage on the corresponding NFC reader antenna will be larger. In the paper, we show how TextileSense leverages this basic property of NFC to detect the presence of nearby objects without knowledge of their orientation, location, and impedance.

3 OVERVIEW

TextileSense aims to detect and locate objects in the proximity of a multiple-coil textile NFC reader. It specifically aims to beamform electromagnetic waves in the near-field to detect the influence of conductive objects.

Approach: TextileSense’s system design is as follows: TextileSense applies different beamforming weights across multiple textile coils of an NFC reader, which can alter the magnetic field to maximize the influence of conductive objects (tagged or untagged) in the near-field. It infers the optimal

set of beamforming weights by measuring the voltage across multiple reader coils. The underlying principle relies on the weak magnetic coupling between the object and the reader coils. As we gradually measure the voltage across multiple coils corresponding to different beamforming weight vectors, we can learn the environment and improve the searching of optimal beamforming vectors to discover various objects in the near-field. Once TextileSense discovers an object, it leverages the voltage measurement on the object’s influence across reader coils with a data-driven model to locate the object.

Challenges: The rest of the paper addresses the key challenges in designing three main aspects of TextileSense:

(1) Optimal Near-Field Beamforming: First, TextileSense needs to measure the wireless channel corresponding to the magnetic coupling of the objects of interest to infer the optimal beamforming vector that can best detect this object. While the channel can be measured indirectly by magnetic coupling, TextileSense needs to detect objects that are outside the range of measurement sensitivity of any single NFC reader coil. Thus, TextileSense must collaboratively process signals across all coils to search for potential objects and amplify the magnetic feedback. While one may measure the channel of each object individually in the far-field, the induced magnetic field across objects can interfere with each other in the near-field. Thus, a key to finding the accurate optimal beamforming vector for each object is to model and estimate the radio environment including the coupling among multiple objects and the influence of undesired ambient conductors. Sec. 4 describes our approach.

(2) Localization in the Near-field: Second, TextileSense should localize the object using the voltage measured across multiple reader coils. At a first glance, we may consider using traditional far-field localization techniques [23, 46]. However, in the near-field, modeling the magnetic field under multiple reader coils is complex and different from the far-field EM modeling. Thus, we propose a near-field localization algorithm, where a data-driven model captures the relationship between the voltage measurement across multiple reader coils and the location of objects while taking the beamforming vectors into account. Sec. 5 details our approach.

(3) Designing Textile Coils for Near-field MIMO: Finally, we explore how TextileSense designs coils that can be embedded in textiles. While TextileSense can improve its performance of localization and coverage by adding more reader coils, one must consider the physical constraints of the total available area to deploy a multi-coil system on the furniture, like on a couch. In addition, TextileSense must account for distortions such as folding and crumpling of the

fabric on which coils are attached. Sec. 6 describes how we mitigate these challenges.

4 NEAR-FIELD BLIND BEAMFORMING

TextileSense provides a near-field MIMO solution that detects the presence of conductive objects whose location, impedance, and orientation are *a priori* unknown. We call this *near-field blind beamforming*, where *blind* denotes the fact that neither do we have prior wireless channel measurements from the objects, nor are we aware of their existence or location. This leads to a chicken-or-egg problem: to beam energy to an object, we need its location, which is precisely what we are aiming to find. Unlike the far-field [44], beamforming weights in the near-field under the NFC context are heavily influenced by the environment, the reader itself, and the presence of conductive objects. In this section, we illustrate how this fundamentally changes our approach to perform blind beamforming.

4.1 Indirect Channel Measurements

In this section, we describe our approach to detect the presence of passive conductive objects. In the far-field, without prior knowledge of the object’s location or wireless channels, the reader would struggle to detect if the object is present or otherwise. In the near-field, however, a reader may detect the presence of a conductive object with no energy source. This is because the object and the reader can magnetically couple with each other. This coupling effect is captured by the mutual inductance between the object and the reader, which is a function of the impedance and location of both the reader and the object. Thus, the mutual inductance plays a role in near-field magnetic channels which is similar to the wireless channel state information in the far-field. We seek to use this information to find the optimal beamforming vector that maximizes the amount of energy delivered to the object. This is critical in improving our location-tracking algorithm given that the amount of energy absorbed by the object gives us important cues about the location of the object (see Sec. 5).

To obtain the optimal beamforming vector to an object, TextileSense needs to measure its near-field magnetic channel (we deal with multiple objects in Sec. 4.3). Consider a team of reader coils (see Fig. 2). Mathematically, let us assume that a team of N reader coils collaboratively beam energy to one nearby object. The voltage induced by the object at the i^{th} reader coil can be written as:

$$V'_{R_i} = m_{T_i} \sum_{k=1}^N m_{T_k} I_{T_k} / Z_R \quad (3)$$

where m_{T_i} is the mutual inductance between the nearby object and the i^{th} reader coil, I_{T_k} is the current in the k^{th} reader

coil and Z_R is the unknown object’s impedance as in the equivalent circuit in Fig. 2(b). In this equation, $\sum_{k=1}^N m_{T_k} I_{T_k}$ is the voltage introduced to the object by all N reader coils, and can be represented by V_R . In other words, the voltage induced at the NFC reader coil is proportional to the mutual inductance, m_{T_i} . Indeed, the magnetic channel m_{T_i} is critical in performing optimal beamforming of energy towards the object. This is because, for optimal beamforming, one needs to apply a set of weights to the current of transmitted signal I_{T_i} which can add up the induced signal V_R constructively at the object. Based on the channel reciprocity, if we know the channel between the object and each reader coil m_{T_i} , one can write the optimal beamforming vector B^* as:

$$B^* = \left[\frac{m_{T_i}^\dagger}{\sum_i |m_{T_i}|^2}, i = 1, \dots, N \right] \quad (4)$$

where \dagger is the conjugate operator.

However, obtaining the magnetic channel m_{T_i} directly from the measured voltage at the reader coil V_{T_i} is not straightforward. The reason is twofold: (1). The voltage induced at a certain reader coil is also influenced by the magnetic channels of other coils. Ideally, one can measure the channel by making all other reader coils open-circuit, then use a known impedance of the object with Eqn. 3 and apply B^* to beamform optimally to the object [12]. However, turning off coils would reduce the voltage and decrease the system’s effective range. (2). We typically do not know the impedance of the object *a priori*, which influences m_{T_i} . The following section details how TextileSense infers the object’s voltage with unknown impedance, location, and orientation.

4.2 Finding Optimal Beamforming Vectors

As explained in the previous section, measuring the precise voltage induced at the objects purely from the voltage at a reader coil is challenging due to several unknowns, such as the impedance of the object and the influence of other coils. However, even in absence of these quantities, we can make the following intuitive observation: if the optimal beamforming vector is used across coils to maximize energy delivered to a specific object, the sum of voltage measured across all reader coils should reach a minimum. At a high level, this is because transferring higher net energy to the object will reduce the net energy available within the readers.

To mathematically see why, we revisit Eqn. 2 and rewrite it by including the mutual inductance between the reader coils. We write the voltage at the i^{th} reader coil as:

$$V_{T_i} = V_{0_i} + \sum_{k \neq i} V_{T_{ik}} - V'_{R_i} = V_{T0_i} - V'_{R_i} \quad (5)$$

where: (1) V_{0_i} is the voltage of i^{th} reader coil when other reader coils are open-circuit and no other objects are present in the near-field, (2) $V_{T_{ik}}$ is the voltage introduced by nearby

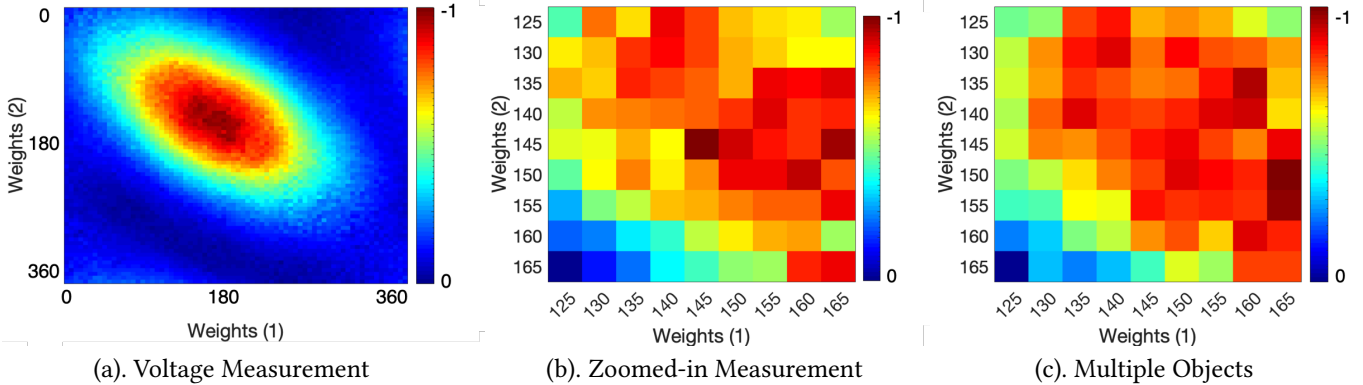


Figure 3: (a) shows the sum of voltage (normalized) measured across three coils when two of them apply different beamforming weights with a step of 5° from 0° to 360°. The global minimum represents the beamforming vector that delivers a maximum amount of power to the nearby object. (b) shows the zoomed-in version in the proximity of the global minimum. (c) shows the voltage measurements when another object is present in the proximity of the target object.

reader coils ($V_{T_{ik}} = m_{T_{ik}} I_{T_k}$, where $m_{T_{ik}}$ is the mutual inductance between the i^{th} reader coil and the k^{th} reader coil). These two components can be calculated as known priors, and we use V_{T0_i} to represent the sum of them. Therefore, it is easy to see that the voltage at the object is maximized when the voltage at the reader is minimized.

At this point, we can formulate an optimization problem that finds the beamforming weights that minimize the net reader voltage. Assume the space of beamforming vectors has J discrete elements B_j ($j = 1, \dots, J$), and $V_{T_i}^j$ ($i = 1, \dots, N$) is the voltage of the i^{th} reader coil when the beamforming vector B_j is applied. Let $V_{T0_i}^j$ be the initial voltage of the i^{th} reader coil when the beamforming vector B_j is applied without any object present. Specifically, we write $V_{T_i}^j = V_{T0_i}^j - V_{R_i}^j$. Our objective is to find the beamforming vector that delivers a maximum amount of energy to the nearby object. Given that we assume only one object is in the near-field for now, we can obtain the optimal beamforming vector as follows:

$$j^* = \arg \min_j \sum_{i=1}^N \|V_{T_i}^j\|^2 \quad (6)$$

Our analysis shows that for arrays of coils, the space of beamforming weights is locally convex. For example, we analyze a three-coil system with one nearby object while applying various beamforming weights across two coils. Fig. 3 plots the sum of the voltage measurement on three coils. It shows a global minimum that delivers maximized energy to the object (see the zoomed-in version in Fig. 3 (b)). Hence, we use Stochastic Gradient Descent to perform the optimization.

4.3 Beamforming to Multiple Objects

While our discussion so far considers only one object in the near-field, this section deals with the case of multiple objects. In traditional far-field beamforming, multiple objects do not pose a problem, since they do not influence each other. However, in the near-field, multiple objects can potentially couple with each other at the same time. TextileSense therefore has to consider multiple objects – if not, the voltage measured from the reader coils will not optimally beam energy to all objects. To see why, we revisit our example in Fig. 3 (b), add another object, and measure again the sum of the voltage across three coils corresponding to different beamforming weights, as shown in Fig. 3 (c). We notice that the consequent voltage map varies considerably from the single-object case.

While prior work in the near-field in wireless charging [37] can charge multiple mobile phones, it does not guarantee to deliver optimized energy to individual receivers; Hence, it cannot guarantee to detect all objects in the near-field.

As a result, TextileSense must account for multiple objects and decouple their influence on the voltage across reader coils. It then finds the optimal beamforming vector for each object in the near-field. We further note that a simple exhaustive search is too time-consuming to be practical. Therefore, TextileSense needs to maximize the total number of objects found under a limited overall time budget.

TextileSense's high-level approach to do so relies on the voltage measurements from multiple reader coils, and it progressively detects objects in the near-field. It then uses this information to update its optimization algorithm.

Discovering Objects: Our approach to discover objects initializes by assuming the presence of a single object in hope of finding a response. We then utilize any response we

receive, particularly from nearby objects to infer the presence of other objects. Specifically, we leverage the fact that the responses from nearby objects are impacted by the coupling between objects that are farther away.

To model the coupling among multiple objects, we revisit Eqn. 3 and rewrite the voltage induced by the object r ($r = 1, \dots, Q$) at the reader coil i when the beamforming vector B_j is applied as:

$$V_{r_i}^{ij} = \underbrace{m_{T_{ir}} \left(\sum_{k=1}^N m_{T_{kr}} I_{T_k}^j \right)}_{\text{induced voltage at the object } r} - \underbrace{\sum_{q \neq r} m_{R_{qr}} I_{T_q}^j}_{\text{voltage from nearby objects}} / Z_r, \quad (7)$$

$$I_{T_q}^j = \sum_{k=1}^N m_{T_{kq}} I_{T_k}^j / Z_q \quad (8)$$

where Z_r and Z_q are the unknown impedance for the object r and q (in their equivalent circuit representations); $I_{T_k}^j$ is the current in the k^{th} reader coil when the j -th beamforming vector is applied; $I_{T_q}^j$ is the corresponding current in the object q ; $m_{T_{ir}}$ is the mutual inductance between the i^{th} reader coil and the object r ; $m_{R_{qr}}$ is the mutual inductance between the object r and the object q . Now, we can write the voltage at the i^{th} reader coil as $V_{T_i}^j = V_{T_{0i}}^j - \sum_{r=1}^Q V_{r_i}^{ij}$ when the beamforming vector B_j is applied.

At this point, we aim to estimate the channel information for each potential object. We set an upper bound Q for the number of potential objects in the near-field. For an N -coil system and R potential objects in the near-field, there are $N * Q$ unknown mutual inductance between the objects and the reader coils, $\binom{Q}{2}$ unknown mutual inductance among the objects, and Q unknown impedance of the objects. While there are $N * Q + \binom{Q}{2} + Q$ unknown parameters, we can resolve them by applying $(N * Q + \binom{Q}{2} + Q)/N$ different sets of beamforming weights since we obtain N equations from each reader coil every time we apply one beamforming vector. For example, with four coils and five potential objects, we need to apply 9 different sets of beamforming weights. While the equations are non-linear, we use Powell's hybrid algorithm [30] to solve them. We evaluate our approach with a four-coil system and four potential objects in Sec. 8.5.

Choosing Beamforming Vectors: There are many possible combinations of beamforming vectors to be applied for estimating the channel of potential objects. TextileSense needs to favor the beamforming vector which delivers a larger amount of energy to these objects. In Sec. 4.2, we formulate an optimization problem to find the beamforming weights that minimize net voltage. TextileSense leverages

the beamforming weights along the gradient to estimate the magnetic channels by solving the non-linear equations.

Improving Object Count Estimates: A key to accurately estimating the potential conductive objects in the near-field is to set an appropriate upper bound of the number of them. TextileSense adaptively tunes the upper bound Q based on the responses from tagged objects in the environment, if available, which provide accurate channel information. We always start estimating the number of objects with an initial Q . If there is no response from a tagged object when we apply the estimated channel for potential objects, we increase Q by one. As we gradually receive responses, we can progressively fine-tune our estimates of these parameters with increasing accuracy. In our experiment, we set the initial value of Q to be 5. With this approach, we can decouple the influence from multiple objects on the voltage of the reader coils and calculate the optimal beamforming vector for each object.

4.4 Tagged vs. Untagged Objects

Telling Apart Tagged vs. Untagged Objects: Untagged objects that are conductive and close to the reader will also couple with our coil antennas. Note that TextileSense models the magnetic channels for both tagged and untagged objects in an identical way. In Sec. 4.3, TextileSense estimates the magnetic channels for all potential objects. With the optimal beamforming, TextileSense can discover them in the near-field. Of these objects, NFC tags actively harvest energy in the near-field and can therefore provide a response. We treat the non-responsive objects as the untagged conductors.

How well can we detect Untagged Conducting Objects? An important factor that decides how well TextileSense can sense a conductive object is how effectively it resonates with the NFC frequency of operation. We note that different shapes, volumes, and materials of conductors lead to various resonant frequencies. For example, water, mobile phones, computer monitors, and even the human body have distinct resonant frequencies. Our NFC signal is at 13.56 MHz, which may not resonate equally well with all classes of objects. Any mismatch lowers the mutual inductance between the reader coil and the object, leading to a small voltage variation at the reader. We explicitly evaluate different classes of conductive objects sensed by TextileSense in Sec. 8.3.

Modeling Fleeting Conductors: While our optimization problem models objects that are static, objects that were computed in the past may no longer exist at the same location in the future. To account for this, TextileSense tracks the magnetic channel of discovered objects. Note that as conductive objects couple with nearby objects, their movement changes the channel of these objects. Thus, TextileSense adaptively tracks the optimal beamforming vectors of the objects based

on the voltage feedback from the reader coils. Specifically, TextileSense monitors the variation of the measured voltage across the reader coils, which indicates that the magnetic channels have been changed. Algorithm 1 presents the details of the complete workflow of TextileSense.

Algorithm 1 TextileSense Algorithm

```

 $\mathbf{B}^* \leftarrow$  Initialized as  $\emptyset$   $\triangleright$  Optimal beamforming set
 $Q \leftarrow$  Initialized as 1  $\triangleright$  Upper bound of potential objects
 $B_1 \leftarrow$  Randomly Initialized Beamforming Weights
Loop:
  1: for  $j = 1, \dots, (N * Q + \binom{Q}{2} + Q)/N$  do
  2:   Apply  $B_j$  to the  $N$  reader coils
  3:    $[V_T^{ij}]_{i=1, \dots, N} \leftarrow$  VOLTMEASUREMENT  $\triangleright$  Sec. 4.1
  4:   if any response from tagged objects (if any) then
  5:     Add the optimal beamforming vector  $B_r^*$  into  $\mathbf{B}^*$ 
  6:      $Q = Q + 1$   $\triangleright$  Tune upper bound
  7:      $B_{j+1} \leftarrow$  UPDATEBEAMFORMERS( $B_j, B_{j-1}$ )  $\triangleright$  Sec. 4.2
  8:   end for
  9:    $\mathbf{B}^* \leftarrow$  OBJECTESTIMATION( $V_T$ )  $\triangleright$  Sec. 4.3
 10:  foreach  $B_r^* \in \mathbf{B}^*, r = 1, \dots, Q$  do
 11:    Apply  $B_r^*$  to the  $N$  reader coils
 12:    Localize object  $r$   $\triangleright$  Sec. 5
 13:  end if
 14: end for
  
```

5 NEAR-FIELD LOCALIZATION

This section describes how TextileSense enables an array of reader coils to locate our objects of interest around the TextileSense-enabled furniture. While TextileSense so far presents a blind beamforming algorithm to detect the objects of interest at unknown locations, it needs to infer their locations with various distances and orientations based on their channel responses. TextileSense leverages an efficient data-driven localization algorithm using the amplitude of the voltage induced across our coil antennas. We choose to model amplitude rather than phase given the low frequency of operation and bandwidth of NFC. Further, the near-field offers more dramatic variations in voltage amplitudes compared to the far-field due to magnetic coupling.

TextileSense's Localization Approach: From our experiments, we find that a near-field multi-coil system like TextileSense exhibits significant coupling effects among its coils, making their individual electromagnetic field diverge from standard path loss models in complex ways; the coupling effects also change with the location, orientation, and impedance of the object of interest. Rather than building a complex analytical model to account for these varying factors, we design a data-driven approach that empirically measures the relationship between the voltage and the objects' location.

We consider the 3-D space within the range of 20 cm and assume all objects of interest will be detected within this coverage with TextileSense's blind beamforming algorithm in Sec. 4. To localize the objects of interest, we measure the voltage across the reader coils with the optimal beamforming weights for a particular object. Our localization algorithm consists of two stages: (1) Designing our empirical model; (2) Performing localization. Below we describe its details.

(1). Designing the Voltage vs. Location Model: We take a data-driven approach and collect the coil voltage V at different object locations as a one-time step prior to the deployment of TextileSense. Specifically, we discretize the space of interest into a 3-D grid with a fixed gap between two consecutive grid points. We carefully select a set of grid points so that they effectively sub-sample our space of interest, and we put objects on these selected points to measure the voltage across all reader coils, after applying the optimal beamforming weights as described in Sec. 4. Note that $V = (v_1, v_2, \dots, v_N)$, where N is the number of reader coils.

Once data is collected, we create a model that maps the voltage measurements V to 3-D locations. We use standard statistical curve/surface fitting methods instead of machine learning models, given that they perform robustly and to avoid overfitting. Theoretically, the strength of the surrounding EM field of an individual antenna is usually modeled to be a fading pattern as the distance increases; traditionally, in the far-field, an antenna is used as a point source. However, these are not true in the near-field, since the communication range of the coil is comparable with the dimension of the coil. For TextileSense, the path loss model varies across different antennas and also within the aperture of individual antennas. Yet, it should still exhibit a certain fading pattern when the distance increases. Thus, TextileSense proposes a two-step fitting model to generate the voltage map in the 3-D space.

First, TextileSense models the path loss with line fitting along the z -axis for individual series of grid points with the same values of x and y (see the red arrows in Fig. 4 (a)). Specifically, the number of curve models corresponds to the number of sample points on the xy -plane. With these curve models, TextileSense is able to estimate V with any z value, i.e., the distance to the coil plane, as long as the point lies on the red arrows in Fig. 4. Our next step is to interpolate V at any point on the 2-D xy -plane grid. This is done by surface fitting (see the blue plane in Fig. 4 (a)). Specifically, we discretize the z -axis with a smaller step size (e.g., 0.1 cm or more fine-grained), and for every z value, we fit a surface given the estimates on the corresponding 2-D grid. By such, TextileSense now effectively stores a bank of $\{(v_1, v_2, \dots, v_N), (x, y, z)\}$ pairs that records the voltage estimates in our space of interest. This can then be used to perform localization. Note that the voltage-to-location model are

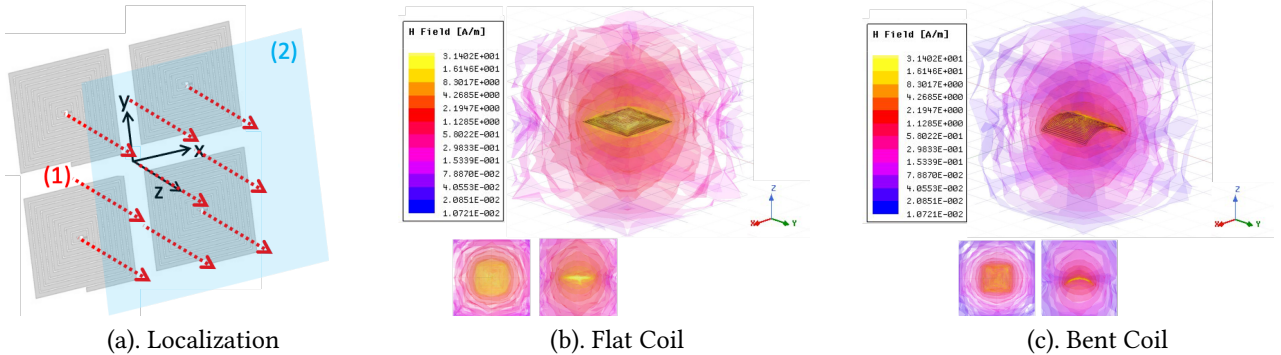


Figure 4: (a) TextileSense’s localization algorithm with four coils. (b) Magnetic radiation pattern of a flat TextileSense coil. The bottom small figures show the radiation strength from Top and Right view. (b) Magnetic radiation pattern of a curved TextileSense coil with 90° bending angle.

only created once before deploying TextileSense. We evaluate TextileSense’s performance under various environments, such as the bending scenario in Sec. 8.2.

(2). Object Localization: To locate the object, we first measure the voltage across the reader coils, and then compare the measurement with the voltage-to-location model to determine the optimal position (x, y, z) based on standard L_2 norm on the voltage vector. We compare this position estimate with the true position of an object when we examine TextileSense’s localization accuracy in Sec. 8.

6 TEXTILE COIL FABRICATION

This section describes our methods to design and fabricate textile coils. Specifically, we discuss: (1). the design of coil pattern that maximizes the radiation characteristics within the constraints of the available area, while remaining robust to bending and crumpling; (2). fabrication methods that integrate textile coils on the furniture.

6.1 Textile Coil Material and Fabrication

Textile Coil Material: There are primarily two types of conductive fabric: (1). intrinsically conductive fibers; (2). non-conductive substrates, which are then coated with an electrically conductive element such as copper and silver. A key trade-off that dictates our choice of conductive fabrics to build our coil antennas is the balance between high conductivity and low parasitic capacitance. Intrinsically conductive fibers have better conductivity; yet, woven conductive fibers tend to have large parasitic capacitance due to the spacing between individual thread of fibers that is negative to the performance of coils. In this case, we choose Nickel-Copper fabric as the conductive textile. This conductive textile sheet

is made of copper and nickel coated nylon ripstop fabric and has an acrylic adhesive layer for a better transfer.

Textile Coil Fabrication: The conductive textile sheet is attached to a 0.4 mm flexible acrylic sheet as the flexible substrate. A laser prototyping system (LPKF U3) is then used to cut the textile sheet into the desired coil shape. The laser scanning parameters are carefully selected to cut through the textile sheet without damaging the acrylic substrate.

6.2 Textile Coil Design

Our objective is to design a coil geometry with an optimized antenna gain within the furniture’s limited area. In this paper, we particularly consider one side of the couch as the designed area to deploy our system (See Fig. 8(d)). To achieve an optimized antenna gain, TextileSense needs to consider the trade-off between the trace width and the number of loops. We model the Q-factor of an inductor to capture the efficiency of our coil antenna. Specifically, the Q-factor can be represented as the ratio of the inductance L to the resistance R of a coil at a given frequency. Note that the inductance and the resistance of the coil antenna is a function of the trace width and the number of loops. We then use the trace width and the number of loops as the unknown parameters to empirically optimize for the Q-factor. Our evaluation shows that the optimal design of the textile coil uses 9 turns of loops, 8 mm trace width of each loop and 2 mm gap between loops. We note that the available deployment area depends on the furniture. Our approach can be used to design the optimal configuration for various sizes of the furniture.

6.3 Textile Bending and Crumpling

Fig. 4 (b) shows the simulated magnetic field of our textile coil without bending (flat). We note that it has high radiation strength and its radiation pattern is perfectly symmetric. However, when the textile coils are deployed on the furniture

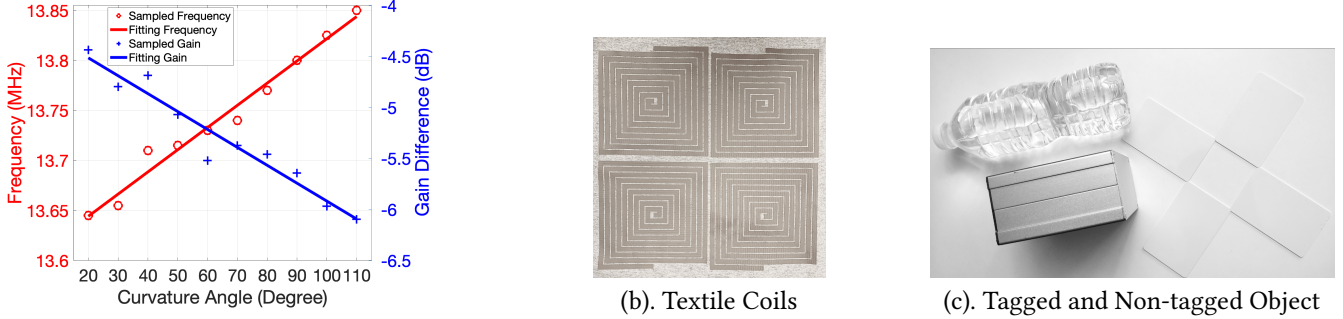


Figure 5: (a) Bending Angle vs. Resonant Frequency / Gain Degradation: As we bend the coil, its resonant frequency shifts higher, and its antenna gain at 13.56 MHz degrades. (b) and (c) show the system components.

like a couch, it may not always remain flat. This section describes the effect of bending and crumpling on TextileSense’s performance, as measured by degradation in antenna gain.

Bending and Crumpling Effect: We first study the impact of bending on TextileSense’s performance when deployed on a couch. We use *bending angle* to model the bending effect. The bending angle can be represented as $\theta = \frac{W}{R}$, where W is the length of the square coil, and R is the radius of an imaginary cylinder to which the antenna is bent. For example, Fig. 4 (c) shows the radiation strength of the coil with 90° bending angle. We notice that the overall radiation strength suffers from degradation due to bending. This is because when we bend the coil antenna, the resonant frequency of the antenna shifts towards a higher frequency, hence the gain of the coil decreases. We then evaluate the resonant frequency shift and the antenna gain degradation across different bending angles from 20 to 110° (see Fig. 5 (a)). We notice that the resonant frequency shift and antenna gain degradation is quasi-linear with different bending angles. We see a 0.2 MHz resonant frequency shift and a 6 dB antenna gain decrease with a 110° bending angle. Also, we model the crumpling of a coil using multiple cylinders with different bending angles. We show that our coil antenna has a 9 dB antenna gain degradation and 0.24 MHz resonant frequency shift when curved by two imaginary cylinders, both with 110° bending angles, from below and above, respectively. TextileSense mitigates the gain degradation by using our near-field beamforming algorithm. In Sec. 8, we evaluate the robustness of our system with certain bending angles.

7 IMPLEMENTATION

NFC Readers and Tags: TextileSense uses four USRP N210 with BasicTX/LFTX daughterboards operating as the NFC reader. We feed one LNA [3] and one customized coil antenna to the antenna port of each USRP. The overall transmitted power of our setup is within FCC regulations. All USRPs are synchronized with the same GPS disciplined clock which

removes the frequency and timing offset among USRPs. We use Mifare Classic 1K tags for tagged object evaluation.

Voltage Measurements: TextileSense measures the voltage of reader coils with commercial available detectors [29] and AD8302 [1]. All detectors connect to an Arduino Due development board with a 12-bit Analog to Digital Converter.

TextileSense Software: TextileSense runs a real-time beamforming search and localization algorithm. It implements an in-house simplified ISO 14443 NFC protocol that can query and apply anti-collision mechanisms to nearby objects in UHD/C++ including phase and amplitude updates. Our source code for the TextileSense algorithm is fully implemented in Python.

Textile Coil Antenna: We designed square coil antennas that resonate at 13.56 MHz. We fabricated coil antennas using Cu/Ni-based conductive textiles. In our evaluation, we use four customized coil antennas which have 9 turns, 8 mm trace width and 2 mm gap (see Fig. 5), and we deploy them on the couch (Fig. 8(d)).

Ground Truth and Baseline: We report accuracy of range and localization in centimeters. To obtain the ground truth, we use a Bosch GLM50 laser rangefinder with an accuracy of 1.5 mm. We also compare TextileSense with two baseline systems: (1) A multi-coil localization based system that does not perform near-field beamforming and instead processes the voltage of individual coils separately. We then use our proposed localization approach as described in Sec. 5 to create a voltage-to-location model for this baseline. We show how this system offers poorer range and localization performance. (2) A large single-coil system that spans the same total area as that of the multi-coil system. Given that this is a single coil system, it cannot perform localization, and can only detect objects. We demonstrate how this system offers poorer detection range due to the inability to beamform.

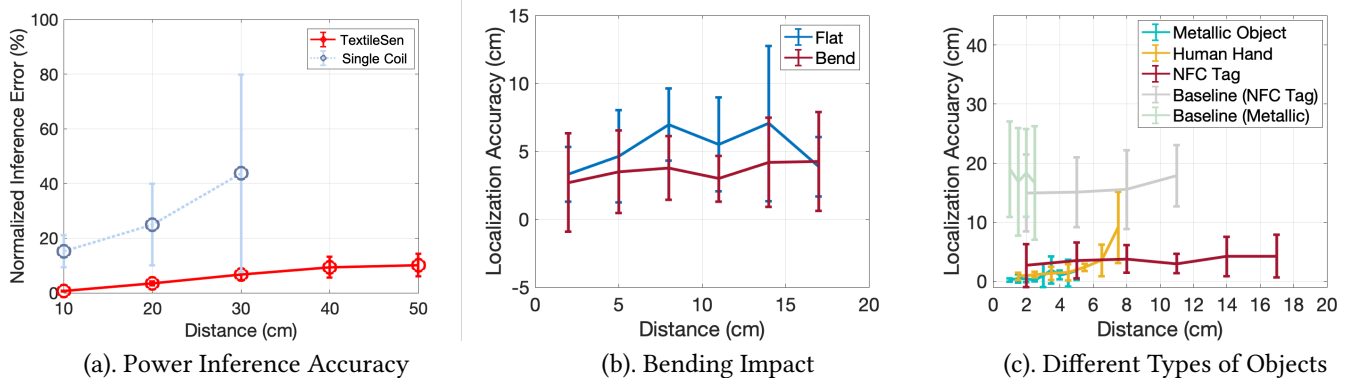


Figure 6: (a) TextileSense infers the power delivered to the nearby objects. The normalized error is the ratio of the error and the ground truth. (b) TextileSense has a better localization performance under the bent scenario than the ideal one. We note that our data-driven system was calibrated only under the bent scenario. In later experiments, we evaluate our system under the bent scenario. (c) TextileSense achieves an average localization accuracy of 3.57 cm, 2.9679 cm, and 0.8956 cm for NFC tags, human hands, and metallic objects respectively.

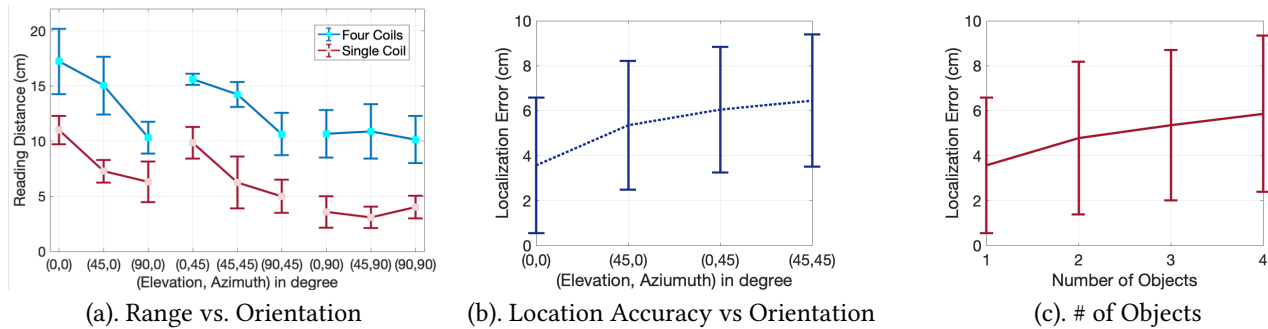


Figure 7: (a) In average, TextileSense shows a $2.04 \times$ detection range compared to a single-coil baseline approach with the same total transmitted power under different object orientations. (b) TextileSense demonstrates its robustness of localization under various object orientations. (c) TextileSense’s localization accuracy when multiple objects are present.

8 RESULTS

8.1 Accuracy of Inferring Power Transfer

Method: In this section, we evaluate whether TextileSense’s beamforming approach can correctly estimate the transferred power to the objects of interest, a key primitive that stems from beamforming and is required for localization. We evaluate the accuracy in inferring the power transferred to the object and compare it to the single-coil system with the same antenna gain and transmitted power. In this experiment, we use four-coil TextileSense to infer the power delivered to one object by measuring the corresponding power induced across all the reader coils. Specifically, we use a receiver coil with a similar impedance and geometry as a potential object (e.g., NFC tag). We then connect the receiver coil to a high-resolution power monitor to obtain our ground truth. We deploy the receiver coil over various locations and distance

up to 50 cm from the reader coils. We infer the power delivered to the receiver coil using TextileSense’s approach: we run the searching algorithm of TextileSense to identify one beamforming vector which delivers the maximum amount of energy to the receiver coil. We then calculate the error in the actual delivered power versus the estimated power, and output the normalized error. For the single-coil system, we assume a known impedance of the receiver coil and calculate the power delivered to the receiver coil directly from the measured power at the reader coil.

Results: Fig. 6 (a) shows the normalized error of estimated power along different distances between the reader coils and the receiver coil for both TextileSense and the single-coil baseline. TextileSense has a mean error of 4.2% in inferring the amount of power delivered to the object. As expected, we notice a gradually increasing power inference error and standard deviation as the distance to the receiver coil increases. We note that our evaluation board has a 12-bit ADC which

could limit the resolution of the measured power. Compared to the single-coil baseline, TextileSense achieves a much higher accuracy of power inference at the same distance. This is because of the gain of beamforming which amplifies minute power variation of the receiver coil even when it is far away from the readers. This helps TextileSense detect the objects in close proximity.

8.2 Localization under Bending

Method: We deploy our system in both the ideal scenario when the coils are flat, and the bent scenario when the coils are bent at 60° . Note that TextileSense takes a data-driven approach to collect the voltage levels at different object locations prior to deployment of the system. We evaluate the localization performance under the ideal scenario and the bent scenario. In the evaluation, we consider NFC-enabled objects.

Results: Fig. 6 (b) shows the localization accuracy of TextileSense under ideal (flat) and bent scenarios. Interestingly, TextileSense has a better localization performance under bending. This is because TextileSense's data-driven system was calibrated only under the bent scenario. While one of the natural limitations of TextileSense's localization algorithm is that its performance degrades when the coil is bent, this drop in accuracy is limited. Overall, TextileSense's approach is robust to significant bending. We note that all remaining experiments are conducted under the bent scenario.

8.3 Tagged vs. Non-tagged Location Accuracy

We evaluate the impact of various types of objects on the localization performance of TextileSense. In the experiments, we consider (1) tagged object: NFC tags, (2) non-tagged object: human hands and a metallic case ($10 \times 8 \times 5$ cm).

Method: We note that, from our experiments, TextileSense can achieve a maximum detection distance of 20.3 cm , 7.5 cm , and 5 cm for NFC tag, human hand, and metallic case, respectively. Thus, we deploy our objects of interest at over 200 various locations within the coverage area of the maximum detection distance. Our goal is to detect the object at unknown locations and estimate its 3-D location using TextileSense's localization algorithm. Further, we compare TextileSense's performance of localizing one NFC-tagged object with a naïve approach (the multi-coil baseline), where each reader coil monitors the voltage individually.

Results: Fig. 6 (c) plots the localization accuracy for different objects with various distances to the reader coils. As we expected, the localization error increases with the distance. Overall, TextileSense achieves an average accuracy of 3.57cm , 2.9679 cm , and 0.8956 cm for NFC tag, human hand,

and metallic case, respectively. We note that TextileSense outperforms the multi-coil baseline, which has significantly poorer detection range (2 and 12 cm for metallic and NFC-tagged objects) and location accuracy (16 cm in average). This shows that in the absence of near-field beamforming, both the detection range and localization accuracy are worse, even if multiple coils are employed.

We note that counter-intuitively, NFC tags have modestly lower localization accuracy compared to human hands. This is owing to each NFC tag's smaller form-factor compared to the other objects considered. We also note that the detection range of the system with untagged objects is lower, given that they do not benefit from the coding gain of NFC tags. We note that the standard deviation of the localization error increases as an untagged object (e.g., human hand) moves farther away from the reader coils, an effect expected due to the degradation of its coupling with the reader coils.

8.4 Impact of Object Orientation

We evaluate the impact of object orientations on the detection distance and localization accuracy of TextileSense. We compare TextileSense's performance with the single-coil baseline that has the same total transmitted power.

Method: We use the reader coil plane as the reference plane and place one object (e.g., an NFC tag) at various locations with different elevation and azimuth angles w.r.t. the reference plane. In our experiments, the initial orientation of the object is facing the reader coil, defined as 0° in elevation and 0° in azimuth. We rotate the object with its elevation and azimuth angle varying from 0° to 90° in steps of 45° .

Results: Fig. 7 (a) and Fig. 7 (b) shows the results of the maximum detection distance and the localization accuracy with different object orientations. We observe that as we rotate the object along the azimuth and elevation, the system performance drops. We note that this is because the cross-sectional area between the reader coils and the object decreases due to its own rectangular form factor. However, our localization error at even the poorest object orientations remains in the range of 2 to 6 cm . Note that we do not report the localization error for the single-coil baseline given that it lacks the ability to triangulate the tag position.

In terms of object detection range, TextileSense significantly outperforms the single-coil baseline by $2\times$. We highlight that TextileSense's extended detection range stems from TextileSense's near-field beamforming solution that alters the distribution of the EM field to deliver maximized energy to the object. From our experiments, we show an average of 14% in relative distance deviation (the ratio of distance deviation to the average distance across various orientations) for TextileSense and an average of 25% relative distance deviation for the single-coil baseline. Hence, TextileSense

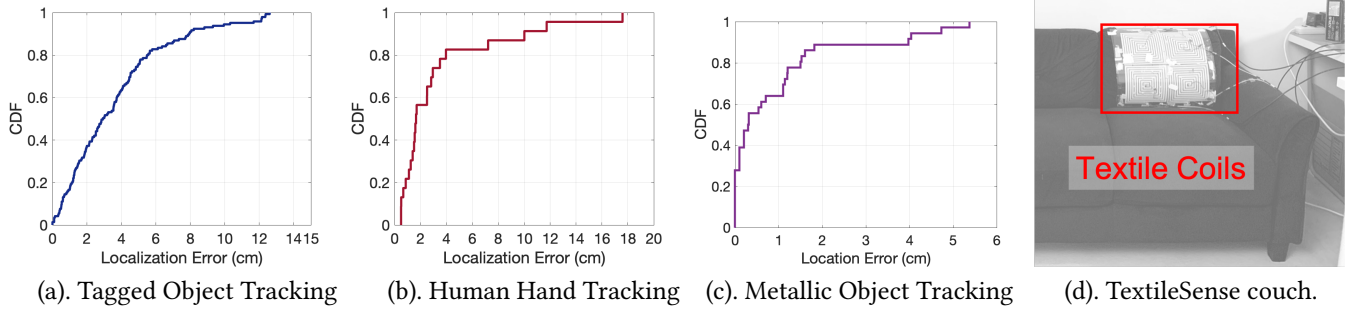


Figure 8: CDF of localization accuracy for (a) NFC-tagged object, (b) human hand, (c) untagged metallic object. (d) Example Application Setup.

has better resilience and stability in the range performance across various object orientations compared to the single-coil baseline.

8.5 Impact of Number of Objects

We evaluate the impact of the number of objects placed in the close proximity on the system performance from two aspects: maximum detection distance and localization accuracy. In the experiment, we use NFC-tagged objects as an example to test the performance, given that the tags' ID will be useful in confirming which and how many objects were identified.

Method: We deploy up to four NFC-tagged objects within a range of 25 cm from the reader coils. We consider various spacings among multiple NFC-tagged objects from 0 (put together) to 30 cm while placed along various orientations.

Results: Fig. 7 (c) shows the mean and standard deviation of the maximum detection distance and the localization accuracy versus the number of NFC-tagged objects. As expected, the mean of detection distance and localization accuracy decreases with more objects (an average of 0.75 cm detection distance and 0.95 cm localization accuracy drop per object). The dip is due to weak coupling among adjacent objects. Yet, the dip is not substantial because TextileSense optimizes the energy delivery one object at a time. The high variance is due to the short spacing among the objects. We observe that TextileSense, in some experiments, achieves a higher-than-expected maximum detection distance when multiple objects are present. We believe this stems from the fact that adjacent objects could act as passive relays to other objects, which allows for better efficiency in energy delivery. We also find that closely packed NFC-enabled objects within 1.5 mm of each other generate strong interference, which makes them struggle to harvest enough energy to make responses. Further, even if they harvest enough energy, their signals are much more likely to collide at the NFC readers.

8.6 Applications

Object Tracking: We show the CDF of the tracking accuracy of tagged and untagged objects in Fig. 8 (a) and (c), respectively. TextileSense is able to locate a tagged object within a median accuracy of 2.84 cm . Consider the case where a wallet/watch is accidentally left on the couch. TextileSense is able to quickly detect this situation through its algorithm and notify the user. Further, our system can potentially support gaming such as augmented and virtual reality where the location of objects needs to be known. We show that TextileSense can detect the location of an NFC tagged plush toy on the TextileSense couch.

User Interface: A TextileSense furniture can be potentially used as a touchless screen, and we evaluate this possibility in Fig. 8 (b). TextileSense can locate a human hand with a median error of 1.53 cm when the user puts his/her hand in close vicinity, making it a promising candidate for touchless screen interfaces. With its ability to locate a human hand, TextileSense can thus track a user's hand once its presence is detected. The user can move his/her hand to form fine-grained gestures, and TextileSense is expected to perform consistent localization to keep tracking and analyzing. We show that the user can finely adjust TV volume by waving the hand over different locations on top of furniture. Here's a video of our system in action : https://youtu.be/Ieil0NQlk_M.

Pose Estimation: TextileSense can also be used to sense the user when the user sits on the couch. Specifically, it can track the location of the user and also the posture of the user. We demonstrate that our system can sense the user's posture – lying or sitting on the couch with 91.3% accuracy.

9 DISCUSSION

Security and Privacy Implications: We note that TextileSense can detect and locate tags as well as objects within close proximity (few tens of centimeters) of the TextileSense furniture. We believe the relatively short range of the system limits privacy risks. We also note that it can facilitate reading

NFC tags at about a four-fold higher distance compared to traditional commercial NFC, which is a potential security vulnerability. While security is beyond the scope of this paper, past solutions [11, 32, 35] that protect NFC tags from malicious scanning can limit the scope of such attacks.

Evaluation of Limitations: We emphasize a few important limitations of our solution: (1) Our evaluation in Sec. 8.5 considers up to four NFC-tagged objects with up to 30 cm of spacing. However, TextileSense cannot deal with extremely small spacing ($< 1.5\text{ cm}$) due to the strong coupling between the objects themselves. (2) TextileSense's performance degrades due to bending, particularly acute bending, as we evaluate in Sec. 8.2, although it continues to perform at an accuracy of few centimeters.

Cost, Power and Scalability: We consider three factors: (1) **Cost:** While we prototype TextileSense using multiple USRPs in this paper, our proposed architecture can be easily adapted to a commercial NFC reader module by using low-cost off-the-shelf phase shifters [2] (less than \$25) and textile coil antennas. (2) **Power:** The power consumption of such a TextileSense system would be less than 100–200 mW, because of the high efficiency of the wireless power transfer in the near-field. (3) **Scalability:** Our evaluation shows TextileSense can detect and localize four NFC tags placed in close proximity. While tag signal collisions might be a potential challenge if there are many NFC tags in the range of TextileSense, the problem can be mitigated using the anti-collision scheme in the NFC protocol that only queries one tag at a time by leveraging the tag's unique ID.

Advantages compared to RFID localization systems: TextileSense supports locating both NFC-tagged objects and untagged conductive objects (e.g., human hand or metal), while traditional RFID localization systems focus on locating RFID tags. Further, TextileSense focuses on an indoor smart home environment where NFC technologies are much more ubiquitous than RFID, such as contactless key fobs, credit cards, ID cards, mobile phones, etc.

10 RELATED WORK

Magnetic Induction: The underlying physics of TextileSense relies on the magneto-inductive principle, which is primarily used as the method for wireless power transfer [5, 41]. Prior work has used relays [7, 10, 20, 38, 39] and multi-antenna systems [12, 37, 45] to improve wireless power transfer based on magnetic induction. Recent work also uses near-field MIMO to improve communication throughput [18]. While past solutions focus on power delivery and channel capacity, we build a practical textile MIMO system in the

commercial NFC context for object localization and user interface for future building infrastructure.

Wireless Sensing: We have seen rich literature on using various wireless technologies to sense our surrounding environment. Past work has proposed Wi-Fi based device-free approach for localization [22], imaging [16], gesture classification [4] and material recognition [48]. Recently, passive RFID tags have been embedded in daily objects like clothing to enable a shape-aware environment [14, 15]. Additionally, recent work [34] proposes locating a customized coil-mounted receiver in the near-field without beamforming optimal energy and therefore operates at very short range (few cm). This paper instead focuses on detecting and locating ordinary conductive objects and NFC-enabled objects in close proximity to the TextileSense furniture.

Smart Fabrics and Materials: Recent work has shown that ordinary fabrics and soft materials are imbued with sensing properties, such as recognizing speech [43], detecting temperature [27], pressure [36], humidity [19], body geometries [28], and activities [13, 17, 26, 31, 33]. Most of these wearable technologies are enabled by connecting off-the-shelf sensors and other circuit components using textile conductive fabrics and threads. Textile antennas for passive NFC and RFID tags [6] are also proposed for body centric and wearable applications. While recent work [9, 42] uses flexible conductive threads for object tracking, the sensing distance for NFC-tagged object is limited up to 3 cm. In contrast, TextileSense builds the first textile MIMO systems for proximate object detection and localization up to 20.3 cm.

11 CONCLUSION

This paper designs TextileSense, an NFC-based system that locates objects (tagged or untagged) in the surroundings using multiple textile coils. TextileSense senses the voltage variation of its transmitter coils induced by proximate objects to detect them and identify their location. We optimize the geometry of the coils and fabricate them to remain robust to fabric bending and crumpling. Through extensive experiments, we demonstrate cm-level localization of both tagged and untagged objects in the near-field.

ACKNOWLEDGMENTS

We thank the members of the WiTech group for their insightful discussions and anonymous reviewers for their constructive feedback. We would like to thank NSF (grants 1942902, 1718435, 1837607, 2030154, and 2007786), CyLab-IoT, the CMU Scott Institute, the Kavcic-Moura grant, and Microsoft Research PhD fellowship for their support.

REFERENCES

[1] 2019. AD8302, Analog Device. <https://www.analog.com/media/en/technical-documentation/data-sheets/ad8302.pdf>.

[2] 2019. Phase Shifters. <https://www.digikey.com/en/products/detail/analog-devices-inc/AD8339ACPZ/1680417>

[3] 2019. ZFL amplifier. <https://www.minicircuits.com/pdfs/ZFL-500LN.pdf>.

[4] Heba Abdelnasser, Moustafa Youssef, and Khaled A Harras. 2015. Wigest: A ubiquitous wifi-based gesture recognition system. In *2015 IEEE Conference on Computer Communications (INFOCOM)*. IEEE, 1472–1480.

[5] Niaz Ahmed. 2017. Magneto inductive communication system for underwater wireless sensor networks. (2017).

[6] Ruben Del-Rio-Ruiz, Juan-Manuel Lopez-Garde, Jon Legarda Macon, and Hendrik Rogier. 2017. Design and performance analysis of a purely textile spiral antenna for on-body NFC applications. In *2017 IEEE MTT-S International Microwave Workshop Series on Advanced Materials and Processes for RF and THz Applications (IMWS-AMP)*. Ieee, 1–3.

[7] Gregor Dumphart, Eric Slottke, and Armin Wittneben. 2017. Magneto-inductive passive relaying in arbitrarily arranged networks. In *ICC*. IEEE, 1–6.

[8] Ramsey Faragher and Robert Harle. 2014. An analysis of the accuracy of bluetooth low energy for indoor positioning applications. In *Proceedings of ION GNSS+ 2014*, Vol. 812. 201–210.

[9] Jun Gong, Yu Wu, Lei Yan, Teddy Seyed, and Xing-Dong Yang. 2019. Tessutivo: Contextual Interactions on Interactive Fabrics with Inductive Sensing. In *ACM UIST*. 29–41.

[10] Burhan Gulbahar. 2017. A communication theoretical analysis of multiple-access channel capacity in magneto-inductive wireless networks. *IEEE Transactions on Communications* 65, 6 (2017), 2594–2607.

[11] Jeremy J Gummesson, Bodhi Priyantha, Deepak Ganesan, Derek Thrasher, and Pengyu Zhang. 2013. EnGarde: Protecting the mobile phone from malicious NFC interactions. In *MobiSys*. 445–458.

[12] Jouya Jadidian and Dina Katabi. 2014. Magnetic MIMO: How to charge your phone in your pocket. In *Proceedings of the 20th annual international conference on Mobile computing and networking*. ACM, 495–506.

[13] Ji Jia, Chengtian Xu, Shijia Pan, Stephen Xia, Peter Wei, Hae Young Noh, Pei Zhang, and Xiaofan Jiang. 2018. Conductive thread-based textile sensor for continuous perspiration level monitoring. *Sensors* 18, 11 (2018), 3775.

[14] Haojian Jin, Jingxian Wang, Zhijian Yang, Swarun Kumar, and Jason Hong. 2018. RF-Wear: Towards Wearable Everyday Skeleton Tracking Using Passive RFIDs. In *Proceedings of the 2018 ACM International Joint Conference and 2018 International Symposium on Pervasive and Ubiquitous Computing and Wearable Computers (UbiComp '18)*. Association for Computing Machinery, New York, NY, USA, 369–372. <https://doi.org/10.1145/3267305.3267567>

[15] Haojian Jin, Jingxian Wang, Zhijian Yang, Swarun Kumar, and Jason Hong. 2018. Wish: Towards a wireless shape-aware world using passive rfids. In *MobiSys*. 428–441.

[16] Chitra R Karanam and Yasamin Mostofi. 2017. 3D through-wall imaging with unmanned aerial vehicles using WiFi. In *2017 16th ACM/IEEE International Conference on Information Processing in Sensor Networks (IPSN)*. IEEE, 131–142.

[17] Ali Kiaghadi, Morgan Baima, Jeremy Gummesson, Trisha Andrew, and Deepak Ganesan. 2018. Fabric as a sensor: Towards unobtrusive sensing of human behavior with triboelectric textiles. In *Proceedings of the 16th ACM Conference on Embedded Networked Sensor Systems*. 199–210.

[18] Han-Joon Kim, Jinho Park, Kyoung-Sub Oh, Jihwan P Choi, Jae Eun Jang, and Ji-Woong Choi. 2016. Near-field magnetic induction MIMO communication using heterogeneous multipole loop antenna array for higher data rate transmission. *IEEE Transactions on Antennas and Propagation* 64, 5 (2016), 1952–1962.

[19] Thomas Kinkeldei, Christoph Zysset, KH Cherenack, and Gerhard Tröster. 2011. A textile integrated sensor system for monitoring humidity and temperature. In *2011 16th International Solid-State Sensors, Actuators and Microsystems Conference*. IEEE, 1156–1159.

[20] Steven Kisseleff, Ian F Akyildiz, and Wolfgang H Gerstacker. 2014. Throughput of the magnetic induction based wireless underground sensor networks: Key optimization techniques. *IEEE Transactions on Communications* 62, 12 (2014), 4426–4439.

[21] Stefan Knauth, Lukas Kaufmann, Christian Jost, Rolf Kistler, and Alexander Klaproth. 2011. The iloc ultrasound indoor localization system at the evala 2011 competition. In *International Competition on Evaluating AAL Systems through Competitive Benchmarking*. Springer, 52–64.

[22] Manikanta Kotaru, Kiran Joshi, Dinesh Bharadia, and Sachin Katti. 2015. Spotfi: Decimeter level localization using wifi. In *Proceedings of the 2015 ACM Conference on Special Interest Group on Data Communication*. 269–282.

[23] Steven Lanzisera, David Zats, and Kristofer SJ Pister. 2011. Radio frequency time-of-flight distance measurement for low-cost wireless sensor localization. *IEEE Sensors Journal* 11, 3 (2011), 837–845.

[24] Filip Lemic, James Martin, Christopher Yarp, Douglas Chan, Vlado Handziski, Robert Brodersen, Gerhard Fettweis, Adam Wolisz, and John Wawrzynek. 2016. Localization as a feature of mmWave communication. In *IWCNC*. IEEE, 1033–1038.

[25] Rong-Hao Liang, Han-Chih Kuo, and Bing-Yu Chen. 2016. GaussRFID: Reinventing Physical Toys Using Magnetic RFID Development Kits. In *CHI (CHI '16)*. Association for Computing Machinery, New York, NY, USA, 4233–4237. <https://doi.org/10.1145/2858036.2858527>

[26] Jaime Lien, Nicholas Gillian, M Emre Karagozler, Patrick Amihood, Carsten Schwesig, Erik Olson, Hakim Raja, and Ivan Poupyrev. 2016. Soli: Ubiquitous gesture sensing with millimeter wave radar. *ACM Transactions on Graphics (TOG)* 35, 4 (2016), 1–19.

[27] Ivo Locher, T Kirstein, and G Tröster. 2005. Temperature profile estimation with smart textiles. In *Proceedings of the International Conference on Intelligent textiles, Smart clothing, Well-being, and Design, Tampere, Finland*. Citeseer, 19–20.

[28] Pasindu Lugoda, Leonardo A. Garcia-Garcia, Sebastien Richoz, Niko Munzenrieder, and Daniel Roggen. 2019. ShapeSense3D: Textile-Sensing and Reconstruction of Body Geometries. In *UbiComp/ISWC '19 Adjunct*. Association for Computing Machinery, New York, NY, USA, 133–136.

[29] Mini-Circuit. 2019. Power Detector. <https://www.minicircuits.com/pdfs/ZX47-40+.pdf>.

[30] Jorge J Moré, Burton S Garbow, and Kenneth E Hillstrom. 1980. *User guide for MINPACK-1*. Technical Report. CM-P00068642.

[31] Chengfeng Pan, Yunsik Ohm, Jingxian Wang, Michael J. Ford, Kitty Kumar, Swarun Kumar, and Carmel Majidi. 2019. Silver-Coated Poly(dimethylsiloxane) Beads for Soft, Stretchable, and Thermally Stable Conductive Elastomer Composites. *ACS Applied Materials & Interfaces* 11, 45 (2019), 42561–42570. <https://doi.org/10.1021/acsami.9b13266> PMID: 31638761.

[32] PITAKA. 2019. MagEZ Wallet. https://www.ipitaka.com/products/magez-wallet?sscid=c1k3_afyov&variant=36583510546

[33] Ivan Poupyrev, Nan-Wei Gong, Shiho Fukuhara, Mustafa Emre Karagozler, Carsten Schwesig, and Karen E Robinson. 2016. Project Jacquard: interactive digital textiles at scale. In *Proceedings of the 2016 CHI Conference on Human Factors in Computing Systems*. 4216–4227.

[34] Vaishnavi Ranganathan, Benjamin H Waters, and Joshua R Smith. 2015. Localization of receivers using phased-array wireless power transfer systems. In *2015 IEEE Wireless Power Transfer Conference (WPTC)*. IEEE, 1–4.

[35] Alpine Rivers. 2019. RFID Blocking Sleeves. www.amazon.com/Blocking-Passport-Protectors-Protection-perfectly/dp/B01F1AGD2C/

[36] Maximilian Sergio, Nicolo Maresi, Marco Tartagni, Roberto Guerrieri, and Roberto Canegallo. 2002. A textile based capacitive pressure sensor. In *SENSORS, 2002 IEEE*, Vol. 2. IEEE, 1625–1630.

[37] Lixin Shi, Zachary Kabelac, Dina Katabi, and David Perreault. 2015. Wireless power hotspot that charges all of your devices. In *MobiCom*. ACM, 2–13.

[38] Kazunobu Sumiya, Takuya Sasatani, Yuki Nishizawa, Kenji Tsushio, Yoshiaki Narusue, and Yoshihiro Kawahara. 2019. Alvus: A Reconfigurable 2-D Wireless Charging System. *Proc. ACM Interact. Mob. Wearable Ubiquitous Technol.* 3, 2, Article 68 (June 2019), 29 pages. <https://doi.org/10.1145/3332533>

[39] Zhi Sun and Ian F Akyildiz. 2012. On capacity of magnetic induction-based wireless underground sensor networks. In *Proceedings of International Conference on Computer Communications*. IEEE, 370–378.

[40] Paul A Tipler and Gene Mosca. 2003. *Physics for scientists and Engineers: Electricity*. WH Freeman.

[41] Andrea Vallecchi, Son Chu, Laszlo Solymar, Christopher J Stevens, and Ekaterina Shamonina. 2018. Coupling between coils in the presence of conducting medium. *IET Microwaves, Antennas and Propagation* (2018).

[42] Nicolas Villar, Daniel Cletheroe, Greg Saul, Christian Holz, Tim Regan, Oscar Salandin, Misha Sra, Hui-Shyong Yeo, William Field, and Haiyan Zhang. 2018. Project zanzibar: A portable and flexible tangible interaction platform. In *CHI*. 1–13.

[43] Jingxian Wang, Chengfeng Pan, Haojian Jin, Vaibhav Singh, Yash Jain, Jason I. Hong, Carmel Majidi, and Swarun Kumar. 2019. RFID Tattoo: A Wireless Platform for Speech Recognition. *Proc. ACM Interact. Mob. Wearable Ubiquitous Technol.* 3, 4, Article 155 (Dec. 2019), 24 pages. <https://doi.org/10.1145/3369812>

[44] Jingxian Wang, Junbo Zhang, Rajarshi Saha, Haojian Jin, and Swarun Kumar. 2019. Pushing the range limits of commercial passive RFIDs. In *NSDI*. 301–316.

[45] Benjamin H Waters, Brody J Mahoney, Vaishnavi Ranganathan, and Joshua R Smith. 2015. Power delivery and leakage field control using an adaptive phased array wireless power system. *IEEE Transactions on Power Electronics* 30, 11 (2015), 6298–6309.

[46] Jie Xiong and Kyle Jamieson. 2013. Arraytrack: A fine-grained indoor location system. In *NSDI*. 71–84.

[47] Lei Yang, Yekui Chen, Xiang-Yang Li, Chaowei Xiao, Mo Li, and Yunhao Liu. 2014. Tagoram: Real-time tracking of mobile RFID tags to high precision using COTS devices. In *Proceedings of ACM MobiCom*. 237–248.

[48] Diana Zhang, Jingxian Wang, Junsu Jang, Junbo Zhang, and Swarun Kumar. 2019. On the Feasibility of Wi-Fi Based Material Sensing. In *MobiCom*. 1–16.

[49] Shilin Zhu and Xinyu Zhang. 2017. Enabling high-precision visible light localization in today's buildings. In *MobiSys*. 96–108.